



## DNN-GFE: A Deep Neural Network Model Combined with Global Feature Extractor for COVID-19 Diagnosis Based on CT Scan Images

---

Javad Hassannataj Joloudari, Faezeh Azizi, Issa Nodehi,  
Mohammad Ali Nematollahi, Fatemeh Kamrannejhad,  
Amir Mosavi, Edris Hassannatajjeloudari and  
Roohallah Alizadehsani

EasyChair preprints are intended for rapid  
dissemination of research results and are  
integrated with the rest of EasyChair.

August 19, 2021

# **DNN-GFE: A Deep Neural Network model combined with Global Feature Extractor for COVID-19 diagnosis based on CT scan images**

**Javad Hassannataj Joloudari<sup>1</sup>, Faezeh Azizi<sup>1</sup>, Issa Nodehi<sup>2</sup>, Mohammad Ali Nematollahi<sup>3</sup>, Fatemeh Kamrannejhad<sup>1</sup>, Amir Mosavi<sup>4,5</sup>, Edris Hassannatajjeloudari<sup>6</sup>, Roohallah Alizadehsani<sup>7</sup>**

<sup>1</sup>Department of Computer Engineering, Faculty of Engineering, University of Birjand, Birjand, Iran

<sup>2</sup>Department of Computer Engineering, University of Qom, Qom, Iran

<sup>3</sup>Department of Computer Sciences, Fasa University, Fasa, Iran

<sup>4</sup>John von Neumann Faculty of Informatics, Obuda University, 1034 Budapest, Hungary

<sup>5</sup>Faculty of Informatics, Technische Universität Dresden, 01069 Dresden, Germany

<sup>6</sup>Department of Nursing, School of Nursing and Allied Medical Sciences, Maragheh Faculty of Medical Sciences, Maragheh, Iran

<sup>7</sup>Institute for Intelligent Systems Research and Innovation, Deakin University, Geelong, VIC 3216, Australia

## **Abstract**

### **Background:**

COVID-19 is a viral disease that was first observed in Wuhan, China in December 2019. This virus can be influenced organs, especially the lungs. The testing kit is one of the most common diagnostics tools for the virus that clinical centers are facing a shortage of due to the increase in patients. Also, X-ray and CT scan images play a crucial role for diagnosing. To the best of our knowledge, artificial intelligence-based methods have been utilized for COVID-19 diagnosis on the images.

### **Materials and Methods:**

Hence, a Deep Neural Network model combined with a Global Feature Extractor called DNN-GFE is proposed for COVID-19 diagnosis with 1252 sick and 1229 Healthy CT scan images. The DNN-GFE model is developed to improve as an accurate diagnostics for classifying Sick and Normal persons. Also, the other classification models such as Decision tree, Random forest, and Neural net had been generated. In this paper, image normalization is used to create good quality images and improve the diagnosis of COVID-19. Furthermore, the 10-fold cross-validation technique is utilized for partitioning the data into training, testing, and validation.

### **Results:**

The experimental results of the DNN-GFE model were compared with three classification models for COVID-19 diagnosis regarding accuracy so that the DNN-GFE model has the most accuracy of 96.71%.

### **Conclusion:**

The proposed model has the best performance regarding evaluation metrics over the existing models that can be utilized instead of a testing kit for COVID-19 diagnosis for clinicians.

**Keywords:** Artificial intelligence, Machine learning, Deep neural network, CT scan images, COVID-19 diagnosis

## 1 Introduction

The coronavirus 2019 (COVID-19) was discovered on December 31, 2019, in Wuhan, China (1, 2). At first, the disease SARS-CoV-2 appeared (3), and later the disease was named Covid-19 (4) by the World Health Organization. The virus has infected more than 40 million persons by October 2020, killing more than one million persons (5). The COVID-19 (6-9) primarily affects the respiratory system and lungs and has Influenza-like symptoms. The rapid and timely diagnosis of covid-19 prevents severe damages to the lungs (10). The most common symptoms of the infectious viral disease include fever, sore throat, cough, weakness, sneezing, lethargy, headache, and respiratory problems (11). One of the most common methods of diagnosing the disease is reverse transcriptase-polymerase chain reaction (RT-PCR), which is expensive and time-consuming (5, 12). The chest X-ray (13-16) is one of the most accessible and cheapest ways of diagnosis, but it is challenging to find covid-19 signals (5). The studies have demonstrated that lung ultrasound has generated more accuracy in diagnosing pneumonia than chest X-ray (17). Seven cases of COVID-19 were reported in the United States on January 20, 2020, with a total of 3963,376 cases of COVID-19 and 143,889 deaths (15). By mid-July 2020, more than 13 million persons had been infected with the disease, and 570,000 had been died (18). That population has increased to 150,779,711 cases of COVID-19 in May 2021 and 3,170,882 deaths (14). In many countries, due to the high growth rate and rapid transmission of coronavirus, social solutions have been considered to prevent the spread of this disease, which include: global lockdown, social distance, closure of schools, universities, shopping malls, travel restrictions, closing borders, etc. These solutions have been caused to reduce the rate of disease transmission and mortality (19). Although image gaining and testing kits are relatively fast and stress-free, analysis of the options can be challenging, costly, and time-consuming for medical professionals in Low-income countries. To resolve these problems, academic researchers have been studied automatic diagnosis methods for the analysis of COVID-19 images based on Artificial intelligence (20). In a study by Berrimi et. al. (21), deep learning methods have been proposed to detect COVID-19. They applied the DenseNet method, the InceptionV3 method, and a novel method called the New-DenseNet method which is obtained by adding a convolutional layer to the DenseNet's architecture. These three methods were used on an X-ray dataset consisting of 1130 X-ray images and a CT scan dataset that contains 2482 CT scans. The highest accuracy was 92.35% for the X-ray dataset while the reported accuracy for the CT scan dataset was 95.98%. Another work that used X-ray scans to detect the infected patients by coronavirus is Sethy et. al. study (22). In this article, the X-ray scans consist of COVID-19, pneumonia, and healthy cases as the three categories. Firstly, fully connected layers of 13 different CNN models extract the deep features of X-ray images and afterward, fed up to SVM to classify each sample according to the aforementioned three categories. Among various models, ResNet50 together with SVM achieved the highest accuracy 95.33%. To classify COVID-19 and healthy X-ray chest images, Ismael & Şengür in (23) proposed a fine-tuned CNN model plus SVM classifier which is applied with several different kernels such as Linear, Quadratic, Cubic and, Gaussian. The dataset which was considered in their work is composed of nearly the same number of COVID-19 (180 cases) and healthy (200 cases) X-ray chest images. The highest accuracy reported among the implemented models was 94.7% obtained by the ResNet50 model and the Linear kernel for the SVM classifier. In (24), two public datasets composed of Pneumonia bacterial, Pneumonia viral, and normal chest X-ray images which together contain 1300 images were considered. The authors implemented a so-called CoroNet model, which is based on Xception architecture, a 71 layer deep convolutional neural network. The regarding method was applied in three different scenarios: the 4-fold CoroNet which was the main model and, two other approaches as modifications. The results of this study show an average accuracy of 89.6%. Shah et. al. in (25), used 738 CT scan images as a dataset for the COVID-19 diagnosis. The authors proposed several models in their study, all of them were based on CNN. At first, a self-constructed model called CTnet-10 was implemented on the data and the result was 82.1% of accuracy. Afterward, to

improve the performance, five other CNN methods were trained on the dataset. Among these models, the VGG-19 model for detecting the positive and negative COVID-19 achieved the highest accuracy of 94.52%. In (26), the authors used two different CT scan datasets for diagnosing COVID-19. On each dataset, they trained different CNN models, transfer learning, and the effectiveness of data augmentation, all built on the SqueezeNet. For every trial, 30 attempts with 20 epochs in each one, were implemented with a various set of hyperparameters. The results show the highest accuracy of 85.03% and 87.55% of sensitivity. In Harmon et al. study (27), a total of 2724 chest CT scans collected from 2617 patients was considered as the dataset. Firstly, utilizing a 3D anisotropic hybrid network (in brief AH-Net), the authors segmented the lung regions of the CT scans. After that, to classify the CT scans, both hybrid 3D and full 3D models were implemented. Finally, by use of a pre-trained DenseNet 121 algorithm, the 3D segmented lung regions were detected and the results show the highest accuracy of 90.8%. In (28), Loey et. al. a total number of 742 CT scan images, consists of 345 COVID-19 cases and 397 healthy ones, considered as the dataset. This study proposed several deep CNN models such as AlexNet, VGGNet16, VGGNet19, GoogleNet, and ResNet50 to diagnose the COVID-19 patients. Also, to improve the models' performance, a combination of data augmentation algorithms and Conditional Generative Adversarial Nets were implemented. The results show that among all of the aforementioned models, ResNet50 has the best performance with an accuracy of 82.91%. Singh et. al. in (29), used the VGG16 model to diagnose patients with Coronavirus infection over 344 COVID images and 358 Non-COVID images collected from three different datasets. At an early stage, as a feature selector, PCA was used and after that, deep CNN, extreme learning machine (ELM), online sequential ELM, and bagging ensemble with SVM were trained on the data as different classifiers. The authors reported the highest accuracy of 95.7% which was obtained by the bagging ensemble with SVM classifier. In this paper, we present four classification methods combined with Global Feature Extractor (GFE) based on CT scan images for automatic COVID-19 diagnosis. The classification methods include Decision Tree (DT), Random Forest (RF), standard Neural Net (NN), and Deep Neural Network (DNN). We have evaluated the efficiency of our methods in terms of accuracy, positive predictive precision, F-measure, Specificity, and Area Under the Curve. Based on the results, the DNN method combined with GFE has the best performance than the other methods. Therefore, the proposed method can be suitable compared to the current testing tools for diagnosing the COVID-19.

The main contributions of the paper are as follows:

- A 6-layer DNN model combined with GFE has been proposed, which has obtained an accuracy of 96.71% for COVID-19 diagnosis.
- A Global Feature Extractor approach has the primary role for feeding data set into modeling that has resulted in a more robust model.
- Construct a lightweight hybrid-DNN model without dropping out on the CT scan images, which has the best performance than the current methods.

## 2 Material and Methods

In this section, the stages of material and methods are described in 2.1, 2.2, 2.3, and subsections. The proposed methodology is shown in Figure 1.

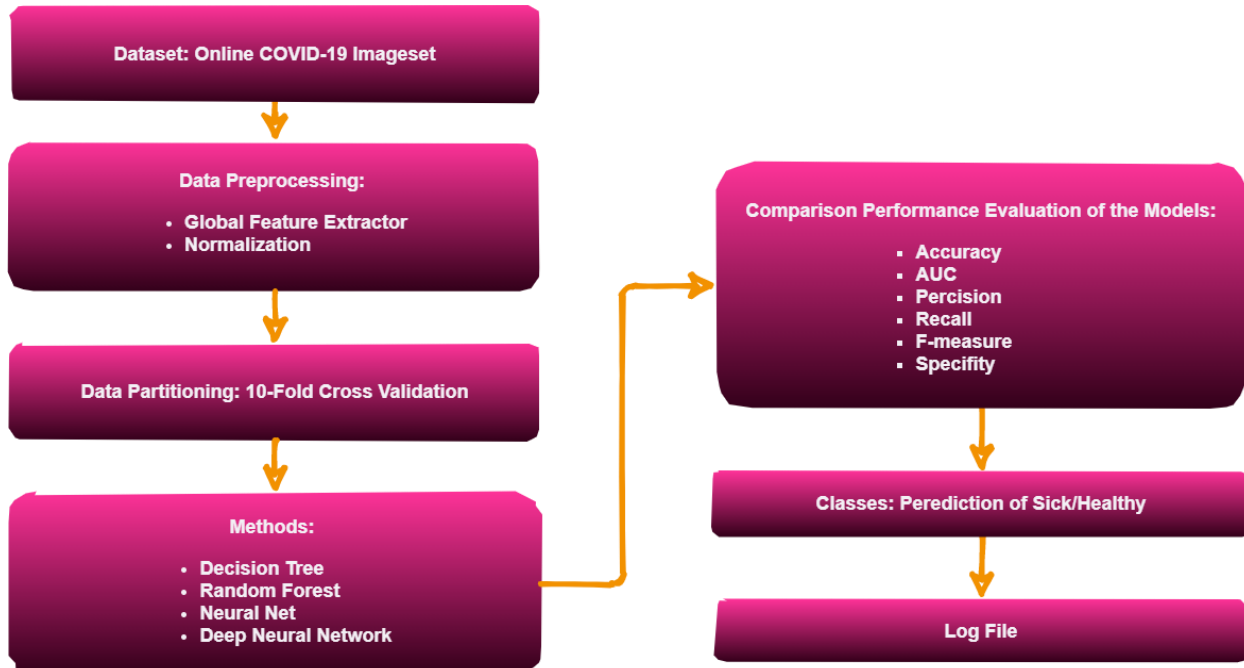


**Figure 1.** The proposed methodology framework.

In this paper, we have used RapidMiner Studio version 9.9 for the COVID-19 diagnosis and classification process.

## 2.1 Data Description

In this paper, we used some of the images for diagnosing sick persons from healthy persons on X-ray images. A brief description of the images is declared in Table 1. Based on Table 1, we observed that the dataset has 1252 sick and 1229 healthy images. The dataset has been extracted from an online source<sup>1</sup>. The two CT scan images from the dataset are illustrated in Figures 2 and 3. The dimensions of the images were different.

**Table 1.** A brief description of the image set.

<u>Class</u>	<u>No. images</u>
Sick	1252
Healthy	1229



**Figure 2.** Sick CT scans.

<sup>1</sup> <https://www.kaggle.com/plameneduardo/sarscov2-ctscan-dataset>

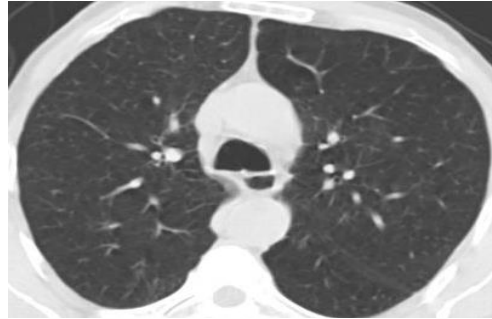


**Figure 3.** Healthy CT scans.

## 2.2 Data Processing

The data processing stage includes Global Feature Extractor (GFE) and normalization of the dataset. First, the multiple color image opener operator is used. It should be noted that the images of the sick and healthy persons are assigned based on the multiple color image opener operator. Following, This operator has a subprocess called GFE from a single image. Using the GFE, feature extraction from a single image is run. Ultimately, the GFE operator has a subprocess that has been comprised of several operators such as global statistics, histogram, and border/interior classification.

Moreover, the images of sick and healthy persons with different dimensions are normalized, which we transformed the images into 100\*100 dimensions. Indeed, dataset normalization is done between zero and one. The normalization approach improves the accuracy of the diagnosis. In other words, this approach reduces the false positive rate. The type of normalization approach, interval transformation, was determined that the images were normalized between zero and one.

## 2.3 Data Partitioning

In this stage, for data partitioning, the k-fold cross-validation (k-FCV) technique, i.e., the dataset is divided into two  $k$  partitions, and the other  $k-1$  partitions are used for training and one partition for testing. In this study, the 10-FCV technique (30) was used for dataset partitioning and executed in each fold by applying 90% of the data for the training and 10% of the remaining data for testing. To handle the training process, avoid data overfitting, improve the generalization, and increase the accuracy, 80% of data had been considered for training and 20% for validation from overall training data in 50 epochs. The process is repeated ten times. Also, the sampling type is selected stratified sampling. The partitioning process through the 10-FCV technique on the data set is shown in Figure 4.

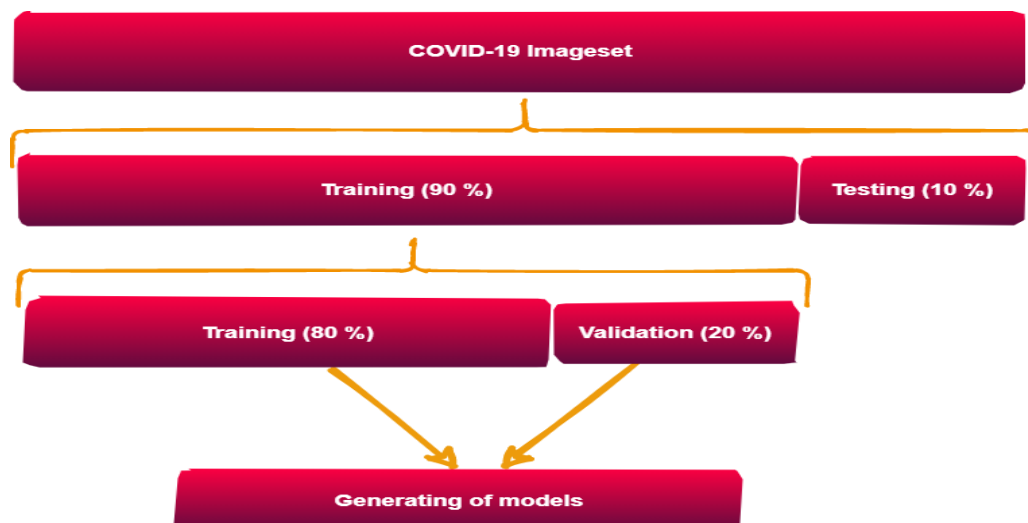


**Figure 4.** Training, testing, and validation process through the 10-FCV technique.

## 2.4 Definition of the Models

### 2.4.1 C5.0 Decision tree

The Decision Tree (DT) is one of the oldest methods of generating a classification model in machine learning. The main idea of the decision tree is to get rules that can aid the specialists in diagnosing the data given by the system. In this paper, the decision tree of C5.0 has been used in the latest creation of the DT models, such as CHAID, ID3, and C4.5 (31, 32). The C5.0 is less time-consuming than the equivalent versions, but it requires a lot of memory. The decision tree is composed of the count of nodes and edges that leaves demonstrate healthy and COVID-19 classes. Also, the decision-making regarding one or several features using the internal nodes is performed. In other words, the C5.0 decision tree is a suitable method due to its simplicity and comprehensibility. Based on the image set, the graphical diagram of the C5.0 decision tree is shown in Figure 5.

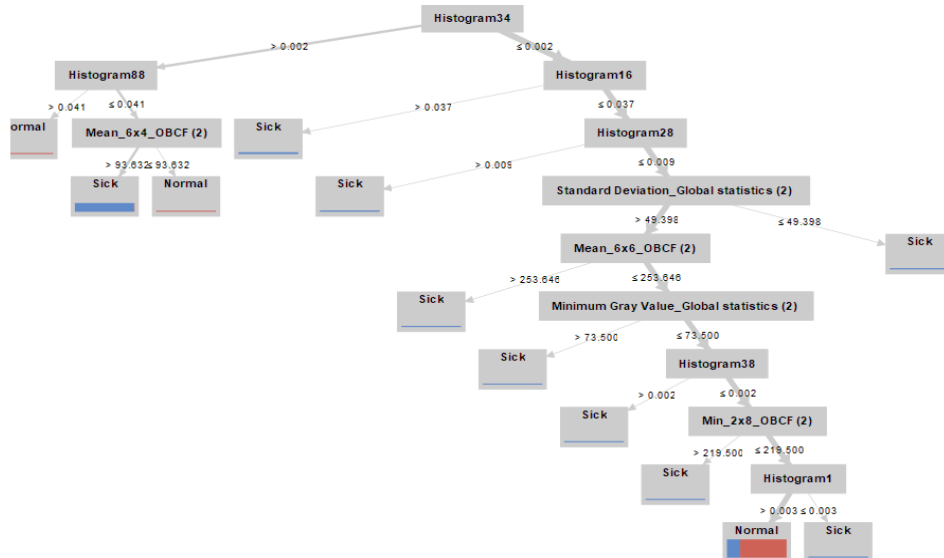


Figure 5. A graphical diagram for the decision tree method combined with GFE.

Moreover, a description of the rule set using the decision tree of C5.0 combined with GFE is illustrated in Figure 6.

```
Histogram34 > 0.002
| Histogram88 > 0.041: Normal {Sick=0, Normal=5}
| Histogram88 ≤ 0.041
| | Mean_6x4_OBCF (2) > 93.632: Sick {Sick=689, Normal=5}
| | Mean_6x4_OBCF (2) ≤ 93.632: Normal {Sick=0, Normal=2}
Histogram34 ≤ 0.002
| Histogram16 > 0.037: Sick {Sick=77, Normal=0}
| Histogram16 ≤ 0.037
| | Histogram28 > 0.009: Sick {Sick=32, Normal=0}
| | Histogram28 ≤ 0.009
| | | Standard Deviation_Global statistics (2) > 49.398
| | | | Mean_6x6_OBCF (2) > 253.646: Sick {Sick=22, Normal=0}
| | | | Mean_6x6_OBCF (2) ≤ 253.646
| | | | | Minimum Gray Value_Global statistics (2) > 73.500: Sick {Sick=14, Normal=0}
| | | | | Minimum Gray Value_Global statistics (2) ≤ 73.500
| | | | | | Histogram38 > 0.002: Sick {Sick=13, Normal=0}
| | | | | | Histogram38 ≤ 0.002
| | | | | | | Min_2x8_OBCF (2) > 219.500: Sick {Sick=10, Normal=0}
| | | | | | | Min_2x8_OBCF (2) ≤ 219.500
| | | | | | | | Histogram1 > 0.003: Normal {Sick=345, Normal=1215}
| | | | | | | | Histogram1 ≤ 0.003: Sick {Sick=8, Normal=0}
| | | | | | | | Standard Deviation_Global statistics (2) ≤ 49.398: Sick {Sick=25, Normal=0}
```

**Figure 6.** A description of the rules generated using the decision tree method combined with GFE on the CT scan images.

The setting up of the parameters of the created DT model is described in Table 2.

**Table 2.** The setting up of the parameters of the DT model

Parameters	Setting
Criterion	Gain ratio
Maximum depth	10
Apply pruning	✓
Confidence	0.1
Apply pre pruning	✓
Minimal gain	0.01
Minimal leaf size	2
Minimal size for split	4
The number of pre pruning alternatives	3

### 2.4.2 Random Forest

One of the robust predictive methods of supervised learning is Random Forest (RF) that which can improve accuracy and speed (31). This method generates various trees and selects the most important votes. Regarding increasing accuracy, it utilizes the assessment of several features and mixes functions. To classify, it puts one input vector to one of the trees in the forest. The structure of the RF on the image set is shown in Figure 7.

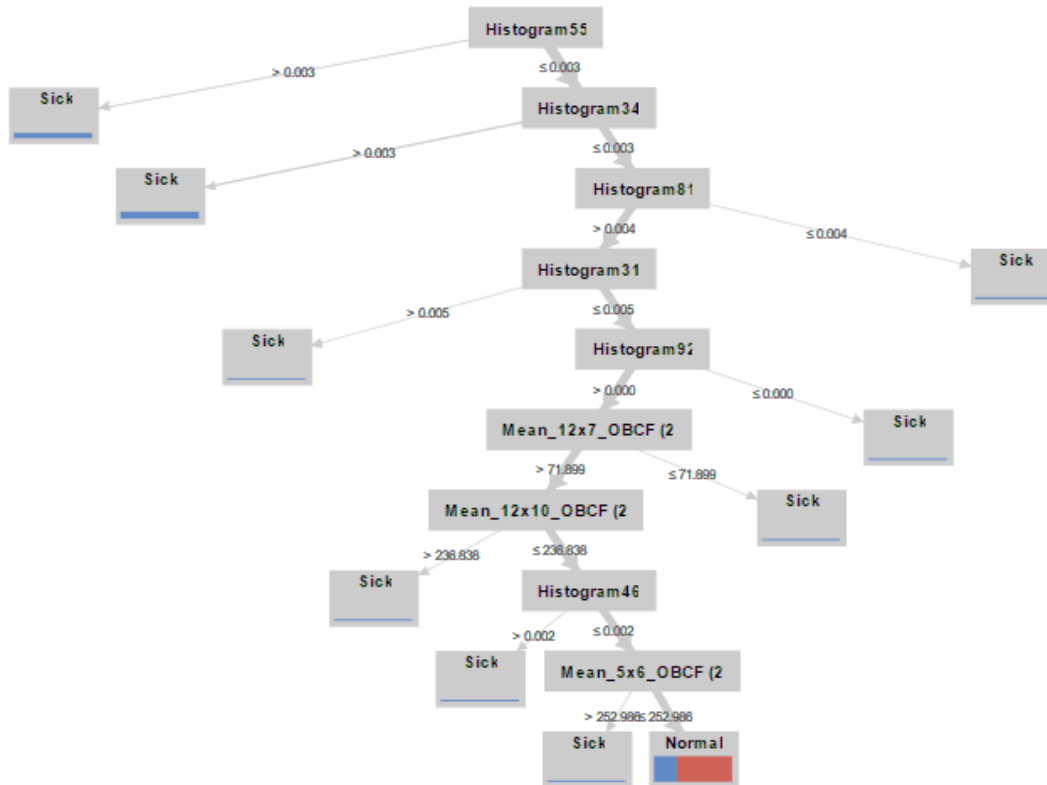


**Figure 7.** A sample of the Random forest method combined with GFE on the CT scan images.

Based on Figure 7, the RF model is better than the decision tree of C5.0 regarding data management, accuracy computing, more information obtain with pruning fewer features, operating with more data, and extracting better rules. So, this model is suitable than the 5.0 decision tree for disease diagnosis. Hence, the RF model can include the following stages:

- I. Using the  $N$  random record in the learning dataset to make the tree.
- II. Each node holds an irregular data sample chosen so that  $b < B$  ( $b$  demonstrates the chosen feature and  $B$  demonstrates the full of features from the dataset. With the growth of trees,  $b$  is kept constant).
- III. Utilizing the  $b$  features chosen for creating the division, the  $P$  node is gained through the best division path from vertexes.  $P$  demonstrate the subsequent node.
- IV. For accumulating, the prediction data utilizes voting through the trained trees with  $n$  trees.
- V. To create the final RF, the model utilizes the most important voted features.
- VI. The RF process terminates when the tree achieves only one leaf node.

Furthermore, a description of the rule set using the RF model combined with GFE is illustrated in Figure 8.

```

Histogram55 > 0.003: Sick {Sick=267, Normal=1}
Histogram55 ≤ 0.003
| Histogram34 > 0.003: Sick {Sick=387, Normal=0}
| Histogram34 ≤ 0.003
| | Histogram81 > 0.004
| | | Histogram31 > 0.005: Sick {Sick=6, Normal=0}
| | | Histogram31 ≤ 0.005
| | | | Histogram92 > 0.000
| | | | | Mean_12x7_OBCF (2) > 71.899
| | | | | | Mean_12x10_OBCF (2) > 236.838: Sick {Sick=10, Normal=0}
| | | | | | Mean_12x10_OBCF (2) ≤ 236.838
| | | | | | | Histogram46 > 0.002: Sick {Sick=24, Normal=0}
| | | | | | | Histogram46 ≤ 0.002
| | | | | | | | Mean_5x6_OBCF (2) > 252.986: Sick {Sick=10, Normal=0}
| | | | | | | | Mean_5x6_OBCF (2) ≤ 252.986: Normal {Sick=495, Normal=1212}
| | | | | | | | | Mean_12x7_OBCF (2) ≤ 71.899: Sick {Sick=3, Normal=0}
| | | | | | | | | | Histogram92 ≤ 0.000: Sick {Sick=11, Normal=0}
| | | | | | | | | | | Histogram81 ≤ 0.004: Sick {Sick=35, Normal=1}

```

**Figure 8.** A description of the rules generated using the Random forest method combined with GFE

In this paper, the setting up of the parameters of the implemented RF model is declared in Table 3.

**Table 3.** The setting up of the parameters of the RF model

Parameters	Setting
Criterion	Gain ratio
Number of trees	20
Maximum depth	10
Apply pruning	✓
Confidence	0.1
Apply pre pruning	✓
Minimal gain	0.01
Minimal leaf size	2
Minimal size for split	4
The number of pre pruning alternatives	3
Guess subset ratio	✓
Voting strategy	Confidence vote
Enable parallel execution	✓

### 2.4.3 Neural Network

The Neural Network (NN) has been generated based on human neurons cells. The neural network contains input and output nodes joined by weighted links. In other words, a multi-layer neural network (33) is specified with three layers; input layer, hidden layer, and output layer. In the input layer, each node is one of the predictive variables, the hidden layer involves weights of nodes, and the output layer represents healthy and sick classes. In general, the input neurons sum and multiply the specified weights of the individually input edge, and by exploiting the bias, the outcome is transformed to an activation function, and its output continues to the subsequent layer (33). The standard neural network is illustrated in Figure 9.

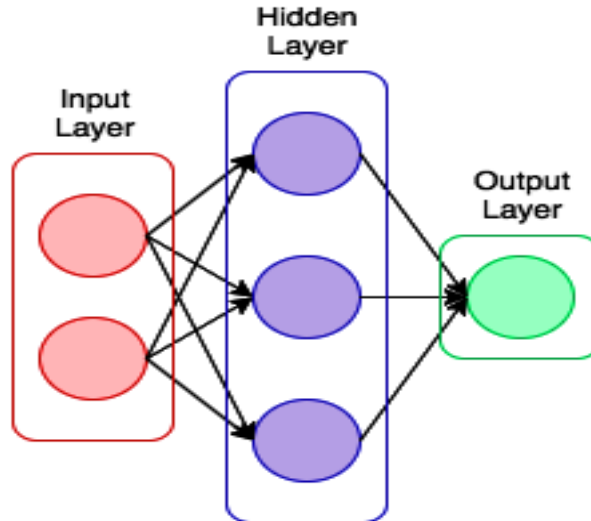


**Figure 9.** A standard neural network model (31, 33).

The setting up of the parameters related to the standard NN model is stated in Table 4.

**Table 4.** The setting up of the parameters of the NN model

Parameters	Setting
Hidden layer sizes	5*2
Training cycles	10
Learning rate	0.01
Momentum	0.9
Shuffle	✓
Normalize	✓
Error epsilon	1.0E-4

### 2.4.4 Deep Neural Network

The Deep Neural Network (DNN) is an improved form of neural network (31). In the DNN model, we encounter multi-layered DNNs, which present multi-layered learning of the features like the essential representative. The layers are titled hidden layers in the NN, and a network is considered a DNN when it contains more than two hidden layers (31). For instance, a DNN model with three hidden layers is shown in Figure 8.

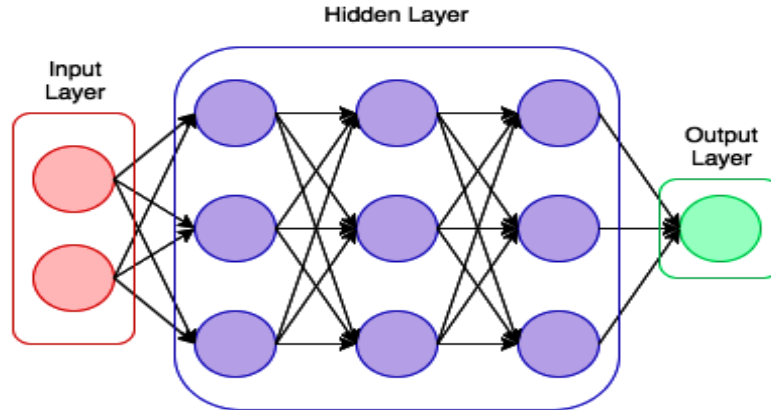


**Figure 8.** A DNN model (31).

Based on figure 8, in a 3-level model (low, middle, and high), more complex features are extracted in the higher layers. The class type of the input data is specified at the model output. Hence, the objective of DNN is to realize some levels of distributed representations of the data by generating features in the lower layers. It can differentiate the options of the variations of the data and then compound these representations in the higher layers. One of the crucial advantages of a DNN model is that this model acts very well on image data and has higher accuracy compared to classification models. Another most significant ability of a DNN is the action to automatically extract features, and it has a high generalization ability to deal with the new data. In this paper, a 6-layer DNN model with four hidden layers sized  $50*30*25*50$  in the 50 epoch scope. Furthermore, the utilized nonlinear activation function, which determines the activity of neurons in the middle layers, is determined by Maxout. The Maxout function chooses the maximum coordinates for the input vector and is used to avoid data overfitting and improve the training of the model. Also, the Softmax function is utilized to classify the output layer of the model. The setting up of the parameters regarding the DNN model is declared in Table 5.

**Table 5.** The setting up of the parameters of the DNN model

Parameters	Setting
Activation function	Maxout
Hidden layer sizes	$50*30*25*50$
Epochs	50
Train samples per iteration	-2
Epsilon	$1.0E-8$
rho	0.99
Standardize	✓
L1	$1.0E-5$
L2	0
Max w2	10
Loss function	CrossEntropy
Classifying	Softmax
Distribution function	Bernoulli

### 3 Results and Discussion

In this section, the results of the methods include the DT, RF, NN, and DNN. Criteria such as accuracy, Positive Predictive Value (PPV), F-measure, Specificity (Spe), and the Area Under the Curve (AUC) have been used to evaluate these methods. These criteria are achieved through a confusion matrix. The confusion matrix is clarified in Table 6.

**Table 6.** Confusion matrix for diagnosis of COVID-19.

The Actual class	The predicted class	
	COVID-19	Healthy
Positive	True Positive	False Positive
Negative	False Negative	True Negative

In Table 6, the factors of the False Positive (FP), False Negative (FN), True Positive (TP), and True Negative (TN) are determined to obtain the following formula (1-4) (33).

- (1)  $Specificity = TN / (TN + FP)$
- (2)  $Accuracy = (TP + TN) / (TP + TN + FP + FN)$
- (3)  $precision = TP / (TP + FP)$
- (4)  $F - measure = 2 * \frac{precision * recall}{precision + recall}$

The performance of the models in terms of accuracy demonstrates that the DNN-GFE model with 96.71% has the best performance compared to the DT-GFE, RF-GFE, and NN-GFE models reaching 84.57%, 85.62%, and 91.43%, respectively. The precision of the proposed DNN, DT-GFE, RF-GFE, and NN-GFE is obtained as 97.64%, 77.23%, 78.47%, and 90.89%, respectively. Also, using the proposed DNN model, the F-measure and Specificity are achieved 96.67%, and 97.65%, respectively which the value of these criteria using the other methods has been less estimated. These results have been gained through 10-FCV on 2481 CT scan images. The experimental results based on the evaluation criteria are assigned in Table 7. Moreover, another important criterion used to determine the performance of the methods is the Area Under the Curve (AUC) criterion. This criterion is obtained via the surface area blue the diagram Receiver Operating Characteristic (ROC) curve. The ROC curve of the DT-GFE, RF-GFE, NN-GFE, and DNN-GFE is illustrated in Figures 9-12, respectively.

**Table 7.** The comparison of the models on the CT scan images.

Methods	ACC(%)	PPV(%)	F-measure (%)	Spe(%)	AUC(%)
DT-GFE	84.57	77.23	86.37	71.17	84.3
RF-GFE	85.62	78.47	87.21	73.11	94.6
NN-GFE	91.43	90.89	91.56	90.18	96.6
DNN-GFE	96.71	97.64	96.67	97.65	99.5

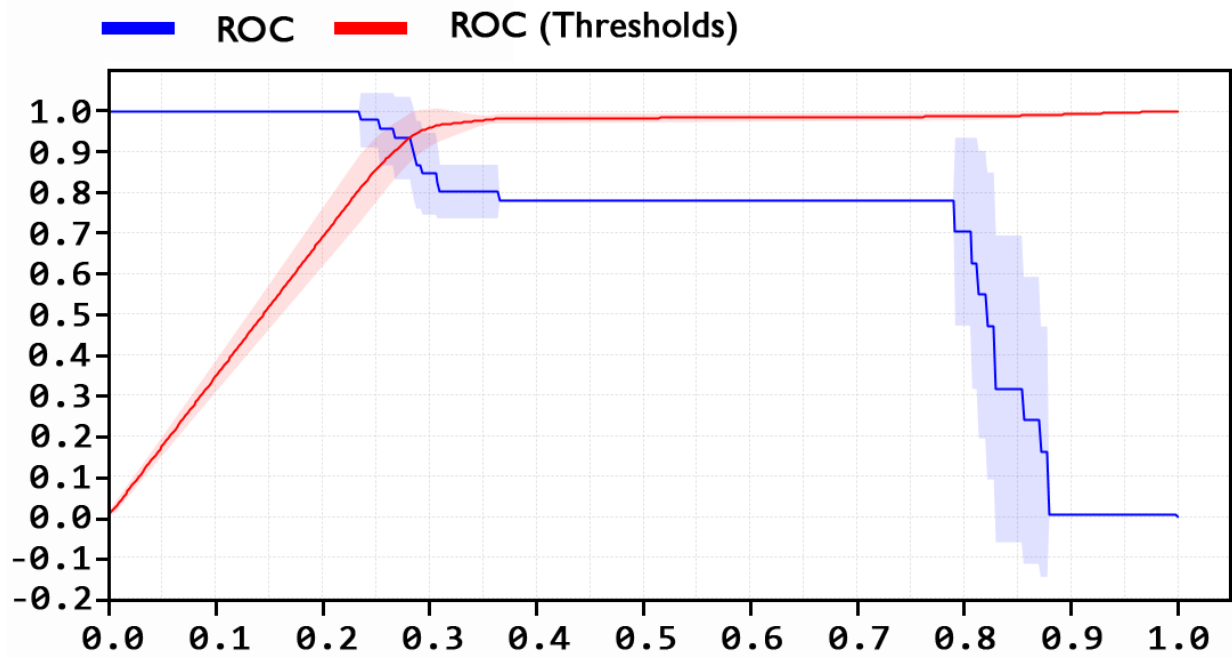


**Figure 9.** The ROC diagram for the Decision tree method combined with GFE on the CT scan images.

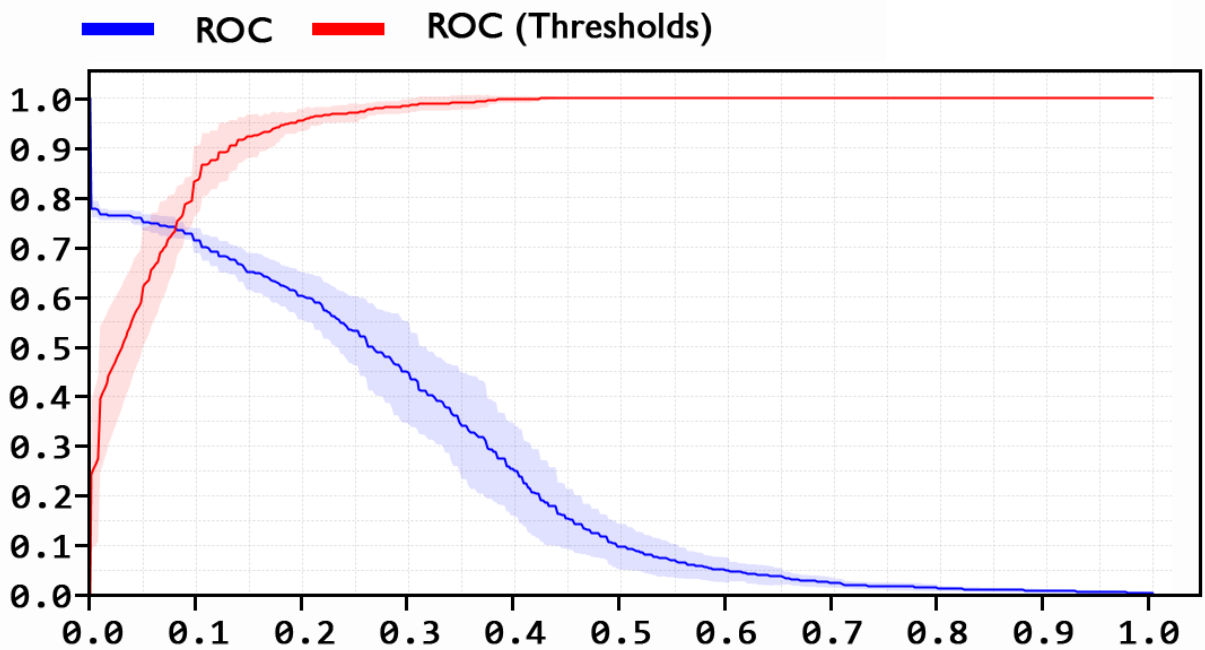


**Figure 10.** The ROC diagram for RF combined with GFE on the CT scan images.

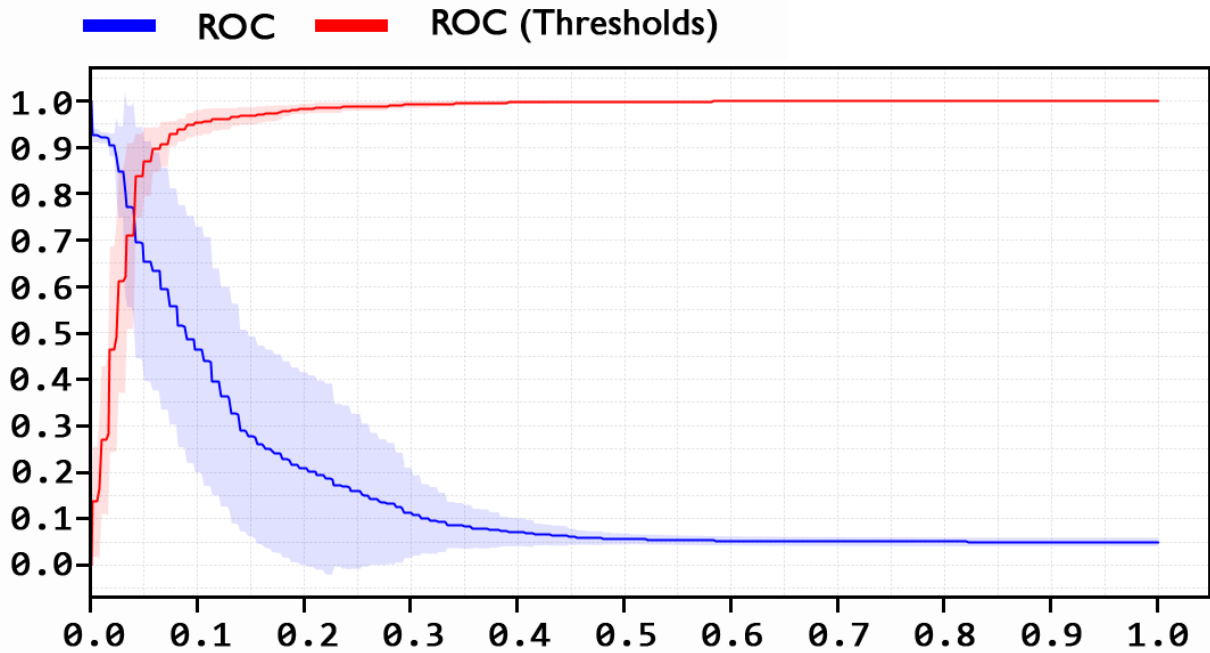


**Figure 11.** The ROC diagram for NN combined with GFE on the CT scan images.

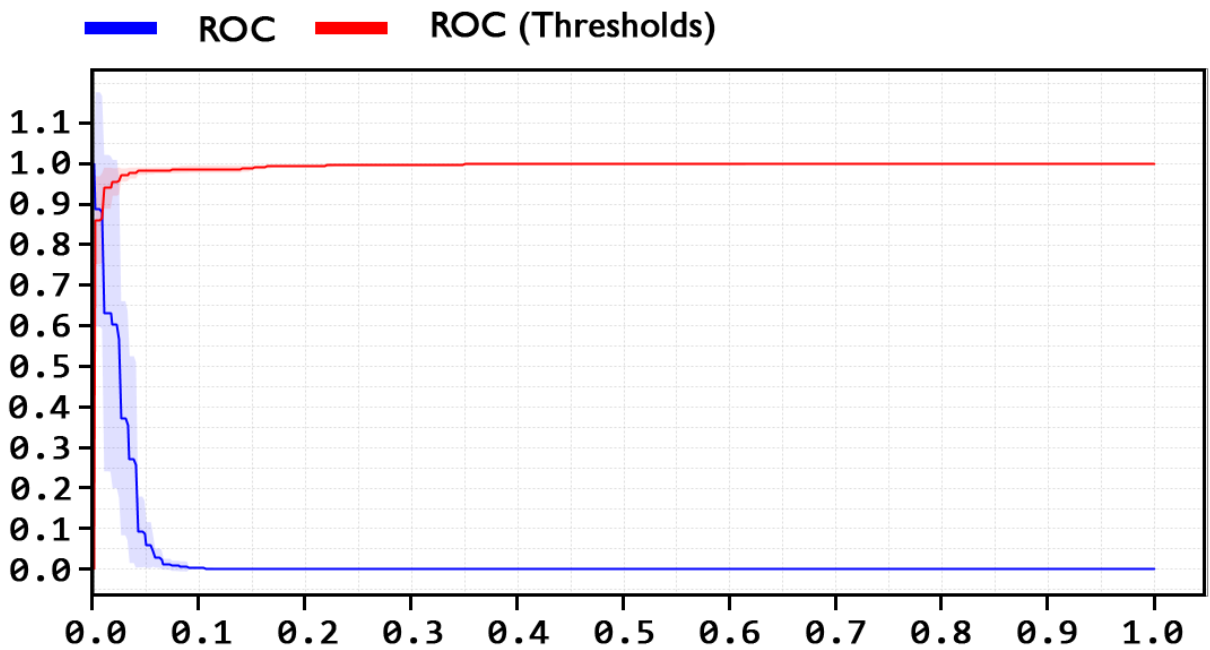


**Figure 12.** The ROC diagram for DNN combined with GFE on the CT scan images.

Based on Figures 9-12, it can be founded that the proposed hybrid model has the best AUC rate of 99.5% than the DT-GFE, RF-GFE, and NN-GFE, reaching 84.3%, 94.6%, and 96.6%, respectively.

Ultimately, a comparison between the DNN proposed method regarding the accuracy achieved on the CT scan images is demonstrated in Table 8.

**Table 8.** Comparison between the proposed DNN-GFE method and the work of other researchers based on the CT scan images.

Authors	Techniques	No.K- FCV	Results
Berrimi et. al (21)	ResNet50 + SVM	NA	ACC: 95.98
Shah et. al. (25)	VGG-19	NA	ACC: 94.52
Polsinelli et. al. (26)	light architecture CNN based on SqueezeNet	10-FCV	ACC: 85.03 Sen: 87.55 Spe: 81.95
Harmon et al. (27)	AH-Net DenseNet121	NA	ACC: 90.8 Sen: 84 Spe: 93 AUC: 94.9
Loey et. al. (28)	ResNet50	NA	ACC: 82.91 Sen: 80.85 Spe: 91.43
Singh et. al. (29)	VGG16 + PCA + Bagging Ensemble with SVM	10-FCV	ACC: 95.7 PPV: 95.8 AUC: 95.8
In this paper	DNN-GFE	10-FCV	ACC: 96.71 PPV: 97.64 F-measure: 96.67 Spe: 97.65 AUC: 99.5

Table 8 reveals that the proposed DNN-GFE method has the best performance in terms of accuracy, PPV, F-measure, specificity, and AUC compared to other methods and the CT scan images. It should be noted that global feature extractor has a significant rule for improving accuracy and other criteria. Moreover, the 6-layer DNN-GFE method is a lightweight method without dropping out the dataset that can be influenced for COVID-19 diagnosis on the low dataset.

#### 4 Conclusions and Future Works

The pandemic of the COVID-19 has changed people's lives, which has caused negative side effects on the public health systems, especially for the international economy. The COVID-19 test kits are utilized for diagnosing the virus. This diagnostic tool is time-consuming, and due to the fast spread of the virus, it cannot be widely available, especially in low-income countries. Recently, Artificial Intelligence methods, including machine learning and deep learning, have been developed for the early diagnosis of the virus by the academic community. Hence, in this paper, we proposed the Deep Neural Network (DNN) combined with Global Feature Extractor (GFE) called DNN-GFE for COVID-19 diagnosis on the CT scan images. The dataset is preprocessed based on GFE and normalization, and data partitioning is run using 10-fold cross-validation to avoid overfitting and the better evaluation of models. The result of the classification accuracy of the proposed model is obtained as 96.71%. In contrast, the accuracy of the combination of the decision tree, random forest, and standard neural network models with GFE is achieved at 84.57%, 85.62%, and 91.43%, respectively. Also, regarding the area under the curve, the proposed model has the best performance reaching 99.5% compared to the other models. At last, we can conclude that the 6-layer DNN-GFE model as a lightweight hybrid model can be a suitable tool for specialists and AI researchers to diagnose COVID-19.

In the future, the proposed method can be used on a large dataset and it is compared to other methods such as evolutionary algorithms, supervised and semi-supervised algorithms.

## Data availability

Publicly available datasets were analyzed in this study. This data can be found here: <https://www.kaggle.com/plameneduardo/sarscov2-ctscan-dataset>

## Author contributions

JHJ, FA, and EN designed the study. JHJ, FA, EN, MAN, and FK wrote the paper. JHJ, FA, EN, MAN, RA, and AM edited the paper. JHJ carried out the software on the dataset. JHJ, FA, and EN generated all figures and tables. All authors have read and approved the final version of the paper.

## References

1. Khozeimeh F, Sharifrazi D, Izadi NH, Joloudari JH, Shoeibi A, Alizadehsani R, et al. Combining a convolutional neural network with autoencoders to predict the survival chance of COVID-19 patients. *Scientific Reports* (2021) 11(1):1-18.
2. Kumar SU, Kumar DT, Christopher BP, Doss C. The rise and impact of COVID-19 in India. *Frontiers in medicine* (2020) 7:250.
3. Guihur A, Rebeaud ME, Fauvet B, Tiwari S, Weiss YG, Goloubinoff P. Moderate fever cycles as a potential mechanism to protect the respiratory system in COVID-19 patients. *Frontiers in Medicine* (2020) 7:583.
4. Reiter RJ, Abreu-Gonzalez P, Marik PE, Dominguez-Rodriguez A. Therapeutic algorithm for use of melatonin in patients with COVID-19. *Frontiers in medicine* (2020) 7:226.
5. Bassi PR, Attux R. A deep convolutional neural network for COVID-19 detection using chest X-rays. *Research on Biomedical Engineering* (2021):1-10.
6. Mahmoudi MR, Baleanu D, Band SS, Mosavi A. Factor analysis approach to classify COVID-19 datasets in several regions. *Results in Physics* (2021) 25:104071.
7. Ayoobi N, Sharifrazi D, Alizadehsani R, Shoeibi A, Gorriz JM, Moosaei H, et al. Time Series Forecasting of New Cases and New Deaths Rate for COVID-19 using Deep Learning Methods. *arXiv preprint arXiv:210415007* (2021).
8. Pak A, Adegbeye OA, Adekunle AI, Rahman KM, McBryde ES, Eisen DP. Economic consequences of the COVID-19 outbreak: the need for epidemic preparedness. *Frontiers in public health* (2020) 8:241.
9. Larsen JR, Martin MR, Martin JD, Kuhn P, Hicks JB. Modeling the onset of symptoms of COVID-19. *Frontiers in public health* (2020) 8:473.
10. Nabizadeh-Shahre-Babak Z, Karimi N, Khadivi P, Roshandel R, Emami A, Samavi S. Detection of COVID-19 in X-ray images by classification of bag of visual words using neural networks. *Biomedical Signal Processing and Control* (2021) 68:102750.
11. Zebin T, Rezvy S. COVID-19 detection and disease progression visualization: Deep learning on chest X-rays for classification and coarse localization. *Applied Intelligence* (2021) 51(2):1010-21.
12. Gomes JC, Masood AI, Silva LHdS, da Cruz Ferreira JRB, Júnior AAF, dos Santos Rocha AL, et al. Covid-19 diagnosis by combining RT-PCR and pseudo-convolutional machines to characterize virus sequences. *Scientific Reports* (2021) 11(1):1-28.
13. Bhardwaj P, Kaur A. A novel and efficient deep learning approach for COVID-19 detection using X-ray imaging modality. *International Journal of Imaging Systems and Technology* (2021).

14. Johri S, Goyal M, Jain S, Baranwal M, Kumar V, Upadhyay R. A novel machine learning-based analytical framework for automatic detection of COVID-19 using chest X-ray images. *International Journal of Imaging Systems and Technology*.
15. Hussain E, Hasan M, Rahman MA, Lee I, Tamanna T, Parvez MZ. CoroDet: A deep learning based classification for COVID-19 detection using chest X-ray images. *Chaos, Solitons & Fractals* (2021) 142:110495.
16. Tabrizchi H, Mosavi A, Vamossy Z, Varkonyi-Koczy AR, editors. Densely Connected Convolutional Networks (DenseNet) for Diagnosing Coronavirus Disease (COVID-19) from Chest X-ray Imaging. *2021 IEEE International Symposium on Medical Measurements and Applications (MeMeA)*; 2021: IEEE.
17. Muhammad G, Hossain MS. COVID-19 and non-COVID-19 classification using multi-layers fusion from lung ultrasound images. *Information Fusion* (2021) 72:80-8.
18. Zivkovic M, Bacanin N, Venkatachalam K, Nayyar A, Djordjevic A, Strumberger I, et al. COVID-19 cases prediction by using hybrid machine learning and beetle antennae search approach. *Sustainable Cities and Society* (2021) 66:102669.
19. Abbasimehr H, Paki R. Prediction of COVID-19 confirmed cases combining deep learning methods and Bayesian optimization. *Chaos, Solitons & Fractals* (2021) 142:110511.
20. Musulin J, Baressi Šegota S, Štifanić D, Lorencin I, Anđelić N, Šušteršič T, et al. Application of Artificial Intelligence-Based Regression Methods in the Problem of COVID-19 Spread Prediction: A Systematic Review. *International Journal of Environmental Research and Public Health* (2021) 18(8):4287.
21. Berrimi M, Hamdi S, Cherif RY, Moussaoui A, Oussalah M, Chabane M, editors. COVID-19 detection from Xray and CT scans using transfer learning. *2021 International Conference of Women in Data Science at Taif University (WiDSTaif)*; 2021: IEEE.
22. Sethy PK, Behera SK. Detection of coronavirus disease (covid-19) based on deep features. (2020).
23. Ismael AM, Şengür A. Deep learning approaches for COVID-19 detection based on chest X-ray images. *Expert Systems with Applications* (2021) 164:114054.
24. Khan AI, Shah JL, Bhat MM. CoroNet: A deep neural network for detection and diagnosis of COVID-19 from chest x-ray images. *Computer Methods and Programs in Biomedicine* (2020) 196:105581.
25. Shah V, Keniya R, Shridharani A, Punjabi M, Shah J, Mehendale N. Diagnosis of COVID-19 using CT scan images and deep learning techniques. *Emergency radiology* (2021) 28(3):497-505.
26. Polsinelli M, Cinque L, Placidi G. A light CNN for detecting COVID-19 from CT scans of the chest. *Pattern recognition letters* (2020) 140:95-100.
27. Harmon SA, Sanford TH, Xu S, Turkbey EB, Roth H, Xu Z, et al. Artificial intelligence for the detection of COVID-19 pneumonia on chest CT using multinational datasets. *Nature communications* (2020) 11(1):1-7.
28. Loey M, Manogaran G, Khalifa NEM. A deep transfer learning model with classical data augmentation and cgan to detect covid-19 from chest ct radiography digital images. *Neural Computing and Applications* (2020):1-13.
29. Singh M, Bansal S, Ahuja S, Dubey RK, Panigrahi BK, Dey N. Transfer learning-based ensemble support vector machine model for automated COVID-19 detection using lung computerized tomography scan data. *Medical & biological engineering & computing* (2021) 59(4):825-39.
30. Joloudari JH, Azizi F, Nematollahi MA, Alizadehsani R, Hassannataj E, Mosavi A. GSVMA: a Genetic-Support Vector Machine-Anova Method for CAD Diagnosis Based on Z-Alizadeh Sani Dataset. EasyChair, (2021) 2516-2314.

31. Joloudari JH, Haderbadi M, Mashmool A, GhasemiGol M, Band SS, Mosavi A. Early detection of the advanced persistent threat attack using performance analysis of deep learning. *IEEE Access* (2020) 8:186125-37.
32. Joloudari JH, Hassannataj Joloudari E, Saadatfar H, Ghasemigol M, Razavi SM, Mosavi A, et al. Coronary artery disease diagnosis; ranking the significant features using a random trees model. *International journal of environmental research and public health* (2020) 17(3):731.
33. Joloudari JH, Saadatfar H, Dehzangi A, Shamshirband S. Computer-aided decision-making for predicting liver disease using PSO-based optimized SVM with feature selection. *Informatics in medicine unlocked* (2019) 17:100255.